

## ESTIMATION OF FLOW DISCHARGE UNDER THE SLUICE AND RADIAL GATES BASED ON CONTRACTION COEFFICIENT\*

H. KHALILI SHAYAN<sup>1\*\*</sup> J. FARHOUDI<sup>2</sup> AND R. ROSHAN<sup>3</sup>

<sup>1,2</sup>Dept. of Irrigation and Reclamation Eng., University of Tehran, P.O. Box 31587-4111, Alborz, Karaj, Iran  
Email: h\_kh\_shayan@ut.ac.ir

<sup>3</sup>Head of Hydraulic Structures Division, Water Research Institute, P.O. Box 16765-313, Tehran, I. R. of Iran

**Abstract**– Sluice and radial gates are common devices used for flow control in hydraulic structures. This paper demonstrates the variation of the contraction coefficient of sluice gates and three types of radial gates (namely, Hard-Rubber, Sharp and Music Note gates) by using Energy and Momentum Equations (EMEs). This paper presents a novel method for estimating the acting force behind these gates under free and submerged flow conditions. A minimum value of the contraction coefficient for sluice gates was obtained under a certain value of relative gate opening. Under a specific condition, Hard-Rubber gates have a larger contraction than Sharp gates, while Music Note gates have the least contraction. It is recognized that the contraction coefficient decreases as the gate lip angle and the gate opening increase. Under submerged flow conditions, the contraction coefficient of sluice and radial gates would be either increased or decreased depending on the level of flow submergence. It is concluded that using the proposed contraction coefficient in estimating the discharge coefficient demonstrates an acceptable accuracy.

**Keywords**– Sluice gate, radial gate, contraction coefficient, discharge measurement

### 1. INTRODUCTION

Sluice gates are devices commonly used for flow control in irrigation canals. Radial gates have a specific arm radius which can affect its discharge coefficient. The design of a radial gate results in every pressure force acting through the center of the imaginary circle, which the gate is a section of, so that all resulting pressure forces act through the pivot point of the gate, thus making its design and construction easier. Consequently, radial gates need smaller lifting forces than sluice gates. They can be used as simple and inexpensive structures for flow measurement with specific accuracy. For this goal, study on sluice and radial gates as measuring structures is needed. Although these structures have simple design procedures and have been used for many years, few studies were reported on their measurement features, especially in submerged flow conditions. Wahl [1] states calibration methods for radial gates in submerged flow conditions are very inaccurate with errors of up to 50%. There have been several studies on the flow characteristics of sluice gates (Henry [2], Rajaratnam and Subramanya [3], Swamee [4], Belaud et al. [5], Lozano et al. [6], Habibzadeh et al. [7], Cassan and Belaud [8]) and radial gates (Metzler [9], Toch [10], Buyalski [11], Tel [12], Clemmens et al. [13], Shahrokhnia and Javan [14], Wahl [1], Shahrokhnia and Javan [15]). It is evident that the exiting flow from these gates is affected by the water surface level both at upstream and downstream of them as well as their contraction coefficients,  $C_c = \frac{y_1}{W}$  (see Fig. 1). Present literature indicates a very small share of studies on the contraction coefficient of sluice and radial gates under free and submerged flow conditions. On the other hand, estimation of the effects of relative

\*Received by the editors April 7, 2013; Accepted January 27, 2014.

\*\*Corresponding author

gate opening and its submergence ratio on the contraction coefficient will help to truly determine the discharge coefficient of the gate as well as its flow parameters such as the Froude number of incoming flow, submergence ratio, energy loss,...under different flow conditions.

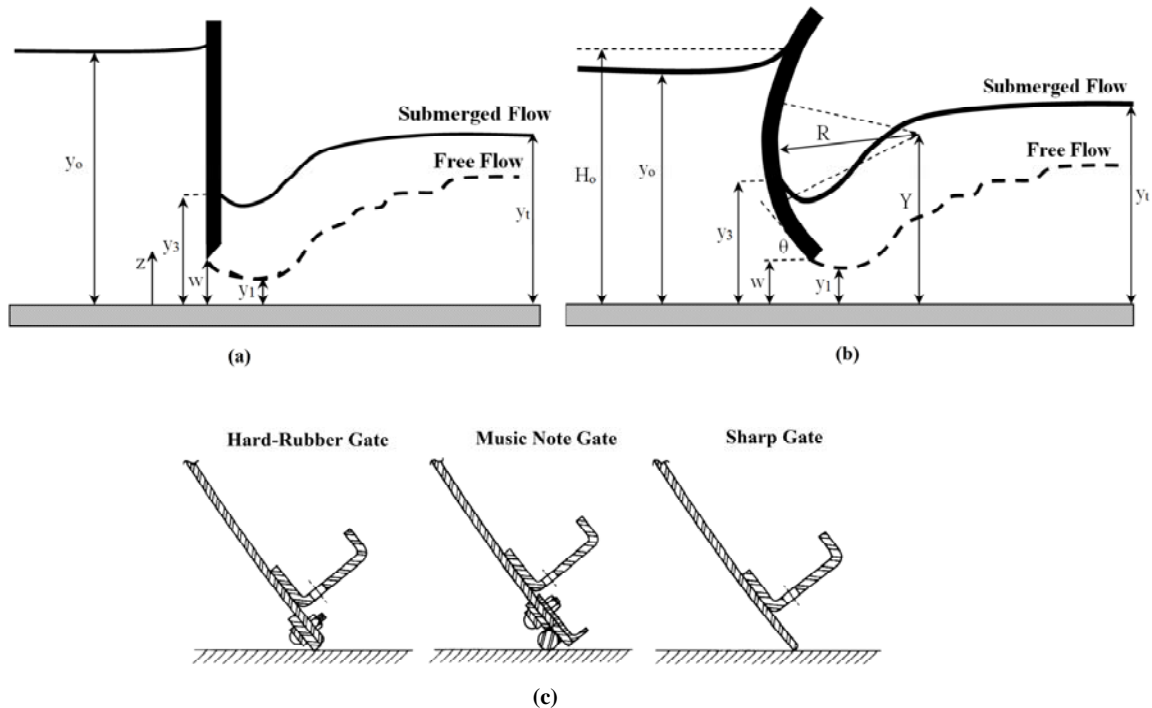


Fig. 1. Definition Sketch for flow under (a) sluice gate, (b) radial gate, (c) different seal types of radial gates (Buyalski [11])

It seems Von Mises [16] pioneered the usage of the flow potential theory to estimate the contraction coefficient of sluice gates. Benjamin [17] conducted experimental studies with two different openings of sluice gates, and measured their contraction coefficient under free and submerged flow conditions. Lin et al. [18] have studied the effective parameters on the contraction coefficient of sluice gates. They considered the reported relationships and experimental data relating to these factors, and presented several graphs showing the contraction coefficient against flow depths at upstream and downstream of a sluice gate. Belaud et al. [5] used the momentum equilibrium and reported a theoretical framework to estimate the contraction coefficient under free and submerged flow conditions. Lozano et al. [6] considered a number of sluice gates in irrigation canals, operating under submerged flow conditions, and found that the effects of the contraction coefficient on the discharge coefficient are considerable at high submergence levels. Cassan and Belaud [8] studied the flow at upstream and downstream of sluice gates, taking benefit from a laboratory layout and two-dimensional numerical simulation of RNG  $k-\epsilon$  (Re-Normalization Group) and RSM (Reynolds Stress Model) turbulence models. They found that the contraction coefficient was increased with high submergence ratios at large gate openings. Ghadampour et al. [19] used the Incompressible Smoothed Particle Hydrodynamics (ISPH) to simulate free-surface mudflow under a sluice gate. They have reported a good agreement between ISPH modeling with experimental data and FVM-VOF results.

Toch [10] suggested an experimental-based equation for variation of the contraction coefficient ( $C_c$ ) with radial gate lip angle ( $\theta^\circ$ ) under free flow condition:

$$C_c = 1 - 0.75\left(\frac{\theta^\circ}{90}\right) + 0.36\left(\frac{\theta^\circ}{90}\right)^2 \quad (1)$$

Tel [12] reported the following equation for the contraction coefficient of sharp radial gates under free flow conditions:

$$C_{c(Sharp)} = 1.001 - 0.2349\theta_r - 0.1843\theta_r^2 + 0.1133\theta_r^3 \quad (2)$$

where  $\theta_r$  is the gate lip angle (in radians). Figure 1. c shows three different seal types of radial gates. Wahl [1] suggested the following relationships for calculating contraction coefficients for Hard-Rubber and Music Note gates, using Buyalski's [11] data which can be written as:

$$C_{c(Hard)} = 0.0138 + 1.0209C_{c(Sharp)} \quad (3)$$

$$C_{c(Music)} = 0.1292 + 0.7884C_{c(Sharp)} \quad (4)$$

It is noteworthy to mention that the relations for estimating the contraction coefficient of radial gates, developed during past decades (Eqs. 1, 2, 3, 4), only consider the effect of the gate lip angle and overlooked the effect of the relative gate opening. This research presents some novel relations to estimate the contraction coefficient of radial gates, considering gate seal type, gate lip angle and relative gate opening as important factors. Moreover, this research extended the E-M method of Belaud et al. [5] for estimating the contraction coefficient of sluice and radial gates under submerged flow condition. The study will employ energy and momentum conservation theories to formulate expressions to determine contraction and discharge coefficients under free and submerged outflow from sluice and radial gates.

## 2. THEORETICAL APPROACH

According to explanations in the previous section, energy and momentum conservation theories are simultaneously used in the following sections to formulate several expressions to determine the contraction coefficient under free and submerged outflow from the gates.

Under submerged flow condition, the forces affecting the control volume, as shown in Fig. 2, are:

- Forces due to hydrostatic pressure, i.e.  $F_{p1}$  and  $F_{p2}$  respectively,
- Forces acting on the upstream and downstream faces of the gate, i.e.  $F_{g1}$  and  $F_{g2}$  respectively,
- The force due to deviation from hydrostatic pressure distribution, i.e.  $F_c$ .

On the other hand, the momentum equation between upstream and downstream of the gate can be expressed as:

$$\sum F_x = \rho q \Delta V_x \rightarrow F_{p1} + F_{g2} + \rho q V_1 = F_{p2} + F_{g1} + F_c + \rho q V_2 \quad (5)$$

$$F_{p1} = \gamma \frac{y_0^2}{2}, F_{g2} = \kappa \gamma \left( \frac{y_3 - w}{2} \right) (y_3 - w) = \kappa \frac{\gamma}{2} (y_3 - w)^2, \rho q V_1 = \frac{\gamma q^2}{g y_0}$$

$$F_{p2} = \gamma \frac{y_3^2}{2}, F_{g1} = \gamma I', \rho q V_2 = \frac{\gamma q^2}{g y_1}$$

where  $\kappa = 1$  for submerged flow,  $\kappa = 0$  in free flow and  $I' = \int_{z=w}^{z=y_0} \frac{p(z)}{\gamma} dy$  is the total pressure head behind the upstream face of the gate with submerged flow.

Rajaratnam and Subramanya [3] suggested a relationship to determine the deviation from hydrostatic pressure at the contracted region as:

$$\Delta p_z = \left(1 - \frac{z}{y_1}\right) \eta \rho \frac{Q^2}{2b^2 y_1^2}, 0 \leq z \leq y_1 \quad (6)$$

where  $\eta$  is approximately 0.08 at a distance  $x=1.25 w$  from the gate. Integrating Eq. (6) results in:

$$dF_c = \Delta p_z B dz = \frac{\eta Q^2 \gamma}{2gb^2 y_1^2} \left(1 - \frac{z}{y_1}\right) B dz \rightarrow F_c = \frac{\eta Q^2 \gamma}{2gby_1^2} \int_{z=0}^{z=y_1} \left(1 - \frac{z}{y_1}\right) dz = \frac{\eta Q^2 \gamma}{4gby_1} \quad (7)$$

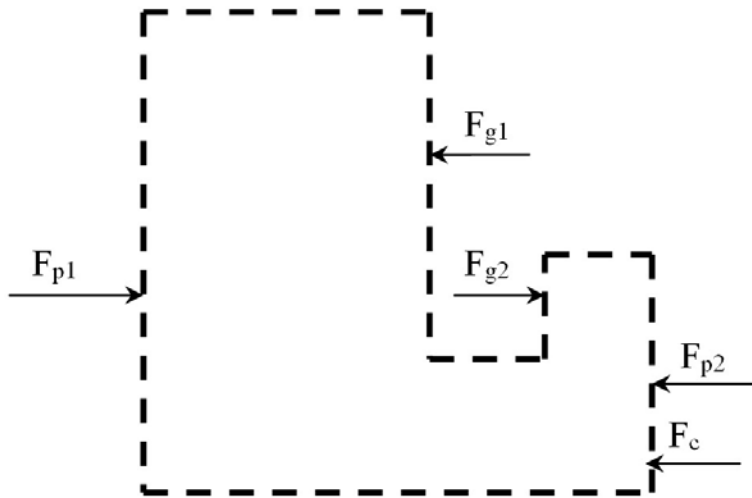


Fig. 2. Effective forces on the control volume before and after the gate

Substituting the above relationships in Eq. (5) results in:

$$\frac{y_0^2}{2} + \frac{\kappa}{2} (y_3 - w)^2 + \frac{q^2}{gy_0} = \frac{y_3^2}{2} + \frac{(\eta + 4)q^2}{4gy_1} + I' \quad (8)$$

Referring to Fig. 1, the energy equation before and after the gate can be expressed as:

$$y_0 + \frac{q^2}{2gy_0^2} = y_3 + \frac{q^2}{2gy_1^2} \quad (9)$$

Defining  $a = \frac{w}{y_0}$  (relative opening),  $s = \frac{y_3}{y_0}$  (relative submergence),  $C_c = \frac{y_1}{w}$  (contraction coefficient),

$C_d = \frac{q}{w\sqrt{2gy_0}}$  (discharge coefficient) and substituting these parameters in Eq. (9), results in:

$$1 + (C_d)^2 a^2 = s + \left(\frac{C_d}{C_c}\right)^2 \quad (10)$$

Calculating the discharge per unit width ( $q$ ) from Eq. (9) and substituting in Eq. (9), and using dimensional parameters, results in a theoretical equation for determining the contraction coefficient under submerged condition, which is related to the relative gate opening, relative submergence and pressure distribution behind the gate and can be expressed as follows:

$$C_c = \frac{\frac{\eta+4}{2}a(1-s) - \sqrt{\left(\frac{\eta+4}{2}a\right)^2 (s-1)^2 - 4\left(\frac{3}{2}a^2 - 2a^2s + sa^3 - \frac{a^4}{2} + a^2\beta'\right)\left(\frac{1}{2} + \frac{a^2}{2} - as - \beta'\right)}}{(3a^2 - 4a^2s + 2sa^3 - a^4 + 2a^2\beta')} \quad (11)$$

in which,

$$\beta' = \frac{I'}{y_0^2} \quad (12)$$

At free flow condition one can define;  $s = C_c a$  and  $\kappa = 0$ . Therefore, Eq. (11) will be shown as:

$$a^3 C_c^3 - 3a^2 C_c^2 + (2\beta + 3)a C_c + (2\beta - 1) = 0 \quad (13)$$

in which  $\beta = \frac{I}{y_0^2}$  and  $I$  is the total pressure head at the upstream face of the gate. The value of  $\beta$  can be determined by using Eqs. (10), (13):

$$\beta = \frac{1 - a^2 C_c^2 + \frac{(C_d)^2 a}{C_c} (4C_c a - 4)}{2} \quad (14)$$

where  $C_c$  is the contraction coefficient which can be defined from Eq. (10) as:

$$C_c = \frac{C_c}{\sqrt{1 + C_c \frac{w}{y_0}}} \rightarrow C_c = \frac{a(C_d)^2 + \sqrt{4 + (C_d a)^2}}{2} \quad (15)$$

Consequently,  $\beta$  can be defined as a function of relative gate opening and discharge coefficient at the free flow condition. Thus  $\beta$  is known if the discharge coefficient and relative gate opening are known.

### 3. RESULTS AND DISCUSSION

#### a) Contraction coefficient of sluice gates at free and submerged flow conditions

Based on their measurements, Roth and Hager [20] suggested the following equation to estimate the effective energy head at the upstream face of the gate at any depth ( $z$ ) from the bed:

$$h_p(z) = 1.538(y_0 - w)(1 - 0.3 \tanh(2.3 \sqrt{\frac{w}{y_0}})) \left[ \left( \frac{z - w}{y_0 - w} \right)^{1/7} - \left( \frac{z - w}{y_0 - w} \right)^{8/7} \right] \quad (16)$$

According to their recommendation, the maximum effective energy head at the upstream face of the gate with free flow can be approximated by:

$$h_{pg(\max)} = (y_0 - w)(1 - 0.3 \tanh(2.3 \sqrt{\frac{w}{y_0}})) \quad (17)$$

Integrating Eq. (17) will give the total effective pressure head at the upstream face of the gate with free flow as:

$$\xrightarrow{\beta = \frac{I}{y_0^2}} \beta \approx 0.62802(1-a)^2(1-0.3 \tanh(2.3\sqrt{a})) \tag{18}$$

Belaud et al. [5] also developed relationships to explain the velocity profiles for outflow from the gates under free flow condition. These relationships help understand the pressure distribution behind the sluice gates. However, from the approach recommended by Belaud et al. [5], one cannot determine a certain value for velocity when  $y=w$ , whereas in the approach proposed by Roth and Hager [20] one can designate a certain value for velocity when  $y=w$ . Therefore, in this work, the proposed equations by Roth and Hager [20] is utilized and justified for submerged flow conditions. Equations recommended by Belaud et al. [5] and Roth and Hager [20] were compared using selected data from Rajaratnam and Subramanya [3] ( $w = 0.0254m, q = 0.06735 \frac{cms}{m}, y_0 = 1.00584m$ ). The result is illustrated in Fig. 3 which shows that the proposed relationship by Belaud et al. [5] resembles hydrostatic pressure distribution.

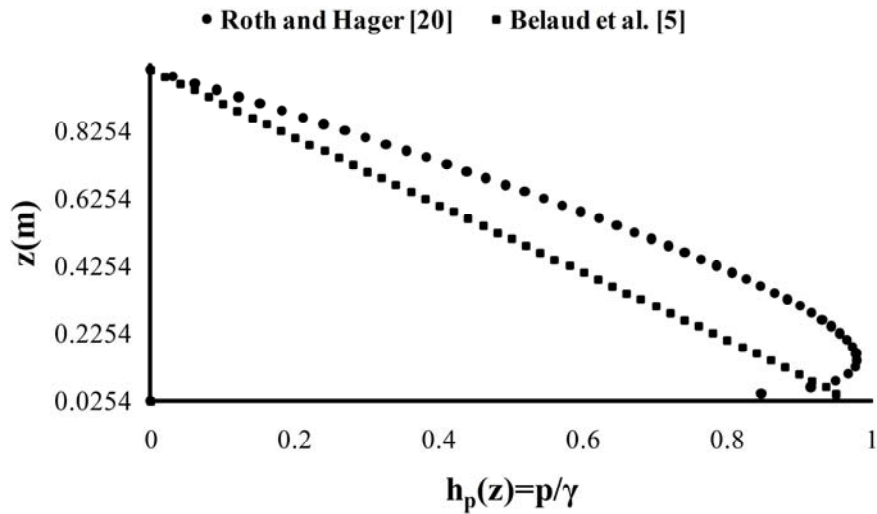


Fig. 3. Comparison between proposed relationships by Belaud et al. [5] and Roth and Hager [20] for distribution of pressure head behind sluice gate

Since there is not enough information on the pressure distribution at upstream face of the gate with submerged flow, one can approximate its value as a product of free flow ( $I' = kI$ ). In this condition, Eq. (8) for determination of  $\beta' = \frac{I'}{y_0^2}$  results in:

$$\beta' = \frac{1+a^2}{2} - sa + (C_d a)^2 - \frac{\eta+4}{2} C_d a \sqrt{1-s+(C_d a)^2} \tag{19}$$

Using Eqs. (18) , (19),  $k = \frac{\beta'}{\beta}$  is defined as:

$$k = \frac{\frac{1+a^2}{2} - sa + (C_d a)^2 - \frac{\eta+4}{2} C_d a \sqrt{1-s+(C_d a)^2}}{0.62802(1-a)^2(1-0.3 \tanh(2.3\sqrt{a}))} \tag{20}$$

By defining an auxiliary parameter  $X$  as:

$$X = \frac{h_{pg(max)}}{y_3} = \frac{h_{pg(max)} / y_0}{y_3 / y_0} = \frac{(1-a)(1-0.3 \tanh(2.3\sqrt{a}))}{s} \tag{21}$$

and using recommendations by Rajaratnam and Subramanya [3] and Cassan and Belaud [8], the variation of  $k$  with  $X$  can be determined (refer to Fig. 4):

$$k = 3.07 - 2.12e^{-0.0174X^{-1.97}} \tag{22}$$

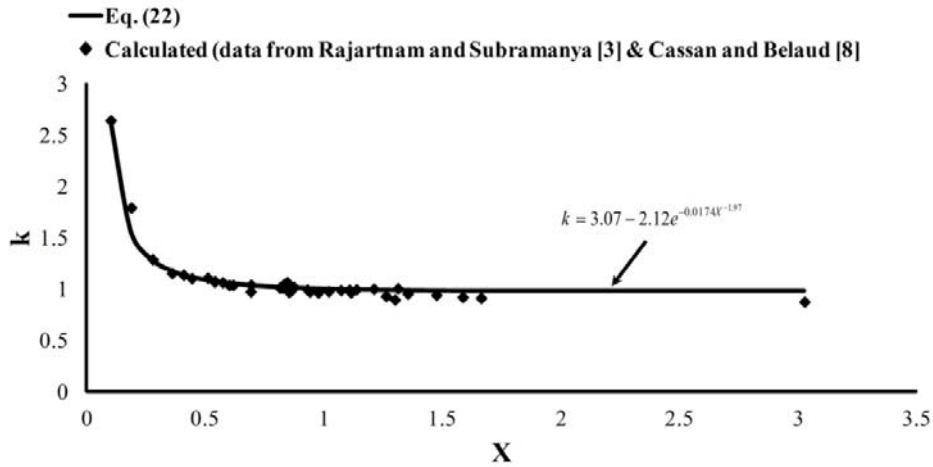


Fig. 4. Variation of  $k$  values with  $X$

It can be observed from Fig. 4 and Eq. (22) that when  $X \rightarrow 1$ , the value of  $k$  approaches unity, which means the pressure distribution at submerged condition falls to its corresponding free flow condition. Variation of contraction coefficient with relative gate opening under free flow condition and the threshold state is shown in Fig. 5. It can be easily observed that the contraction coefficient descends to a minimum value at  $\frac{w}{y_0} \approx 0.6$  and then increases from thereafter, which is in accordance with Belaud et al. [5]. However, the lowest value of contraction coefficient in their work occurs at  $\frac{w}{y_0} \approx 0.4$  instead of  $\frac{w}{y_0} \approx 0.6$ . Figure 5 shows that the contraction coefficient retains a smaller value when a repelled jump occurs. It can also be seen that the contraction coefficient is higher at the threshold state of the gate compared to the free hydraulic jump.

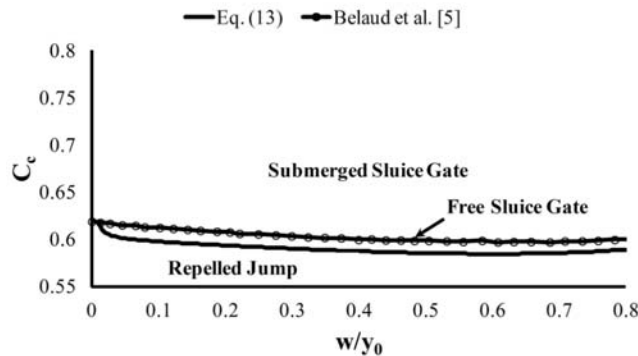


Fig. 5. Variation of calculated contraction coefficient with relative opening of the gate under free flow condition

Figure 6 shows variation of the contraction coefficient with relative opening and relative submergence under submerged flow conditions. It is shown that the contraction coefficient can be increased or decreased with relative submergence. At low submergence levels ( $s = 0.2$  to  $s = 0.5$ ), the contraction coefficient decreases with relative submergence and increases for high submergence levels ( $s = 0.5$  to  $s = 0.9$ ). As the flow becomes submerged, the force due to water weight over the contracted section increases and the thickness of *vena contracta* decreases. This is a dominant factor at low

submergence levels. On the other hand, as the flow becomes more submerged, the difference between water levels at upstream and downstream of the gate decreases, and the output velocity under the gate will also decrease, which results in an increase of the thickness of *vena contracta* and the contraction coefficient which will be more effective at submergence levels.

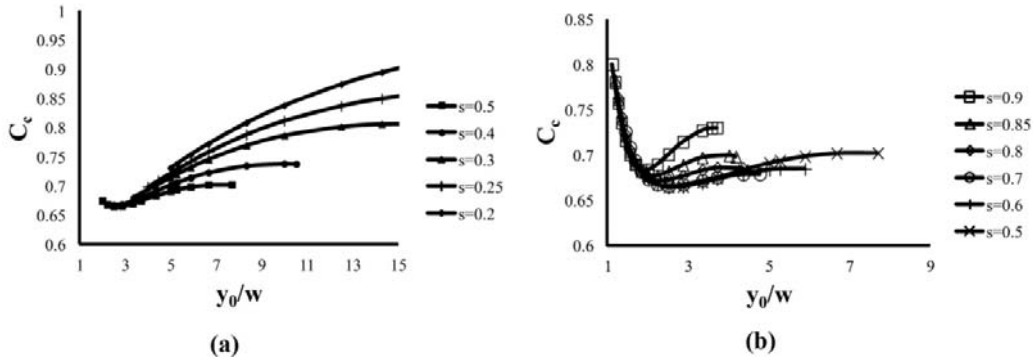


Fig. 6. Variation of calculated contraction coefficient with relative gate opening and relative submergence under submerged flow condition (a)  $s = 0.2 - 0.5$ , (b)  $s = 0.5 - 0.9$

The contraction coefficient can be used for estimating the discharge coefficient at free and submerged flow.

$$C_d = C_c \sqrt{\frac{1-s}{1-C_c^2 a^2}} \tag{23}$$

The accuracy of Eq. (23) was assessed using the data retrieved by Rajaratnam and Subramanya [3] which was conducted on a sluice gate with 45.72 cm in width (refer to Fig. 7). The maximum relative errors in estimating the discharge coefficient are 2% and 4% under free and submerged flow conditions, respectively ( $\%RE = \frac{C_{di(exp)} - C_{di}}{C_{di(exp)}} \times 100$ , where  $C_{di(exp)}$  is the experimental discharge coefficient and  $C_{di}$  is the discharge coefficient calculated by Eq. (23)).

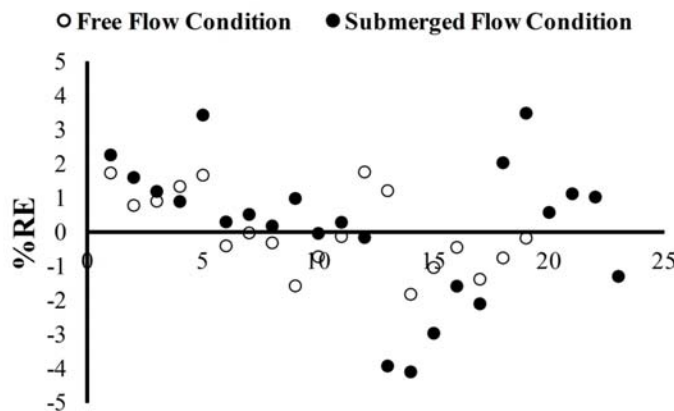


Fig. 7. Evaluation of proposed equations for estimation discharge coefficients in free and submerged flow conditions (Rajaratnam and Subramanya [3])

Another investigation for evaluating Eq. (23) was conducted based on experimental data extracted by Sepulveda [21] which were taken from a number of sluice gates with 43.4 and 44 cm widths. Figure 8 shows that Eq. (23) closely relates the discharge coefficients to experimental values.

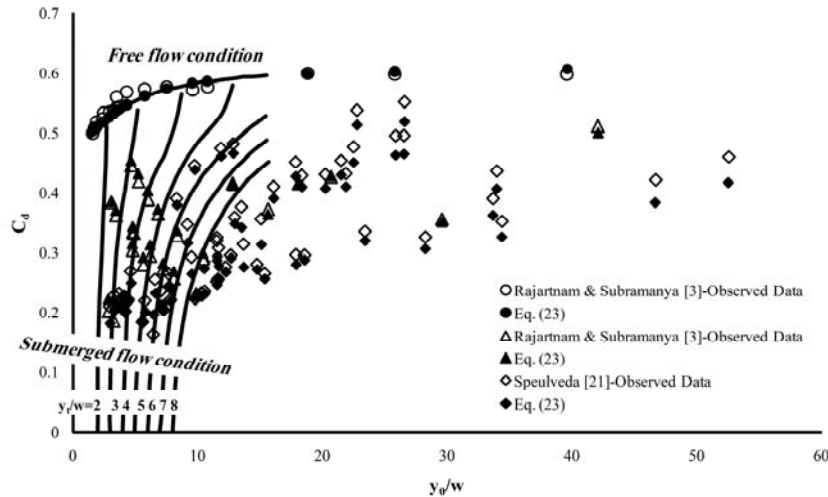


Fig. 8. Evaluation of different methods for estimation of discharge coefficient (Rajaratnam and Subramanya [3] and Sepulveda [21])

**b) Contraction coefficient of the radial gate under free and submerged flow conditions**

For free flow under radial gates, values of  $\beta$  are calculated from Eqs. (14) and (15). In Fig. 9, variation of  $\frac{\beta}{\theta_r}$  with  $\frac{a}{\theta_r}$  for three gate types are depicted, using the data retrieved from Buyalski [11]. Buyalski [11] performed an extensive experimental work on radial gates under free and submerged flow conditions. He used a radial gate in nine different configurations of gate seal types and trunnion pin heights, as shown in Table 1. For all experiments, the gate arm radius was 702 mm while the gate width was 711 mm. Buyalski [11] performed his experiments under three different flow conditions, described as FREE, SUBMERGED and JUMP (assumed as a transitional point).

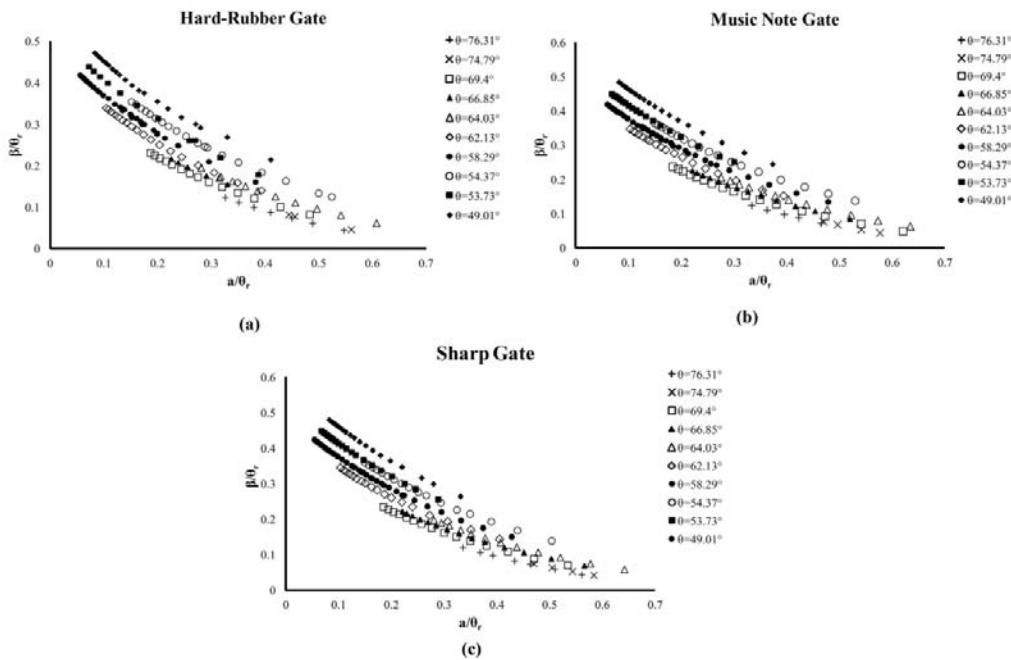


Fig. 9. Variation of  $\frac{\beta}{\theta_r}$  with  $\frac{a}{\theta_r}$  for three types of the gate at free flow condition

Table 1. Radial gate configurations tested by Buyalski [11]

Gate Number	Seal Type	Trunnion-pin height (Y(mm))	Number of Tests
1	Hard-Rubber	461	1108
2	Hard-Rubber	511	380
3	Hard-Rubber	409	420
4	Music Note	409	155
5	Music Note	461	131
6	Music Note	511	119
7	Sharp Gate	409	167
8	Sharp Gate	461	134
9	Sharp Gate	511	118

It can be seen from Fig. 10 that these variations follow a power trendline:

$$\frac{\beta}{\theta_r} = m e^{n \frac{a}{\theta_r}} \tag{24}$$

where  $m, n$  depend on gate seal type and gate lip angle:

$$m = A \theta_r^B, n = C \theta_r \tag{25}$$

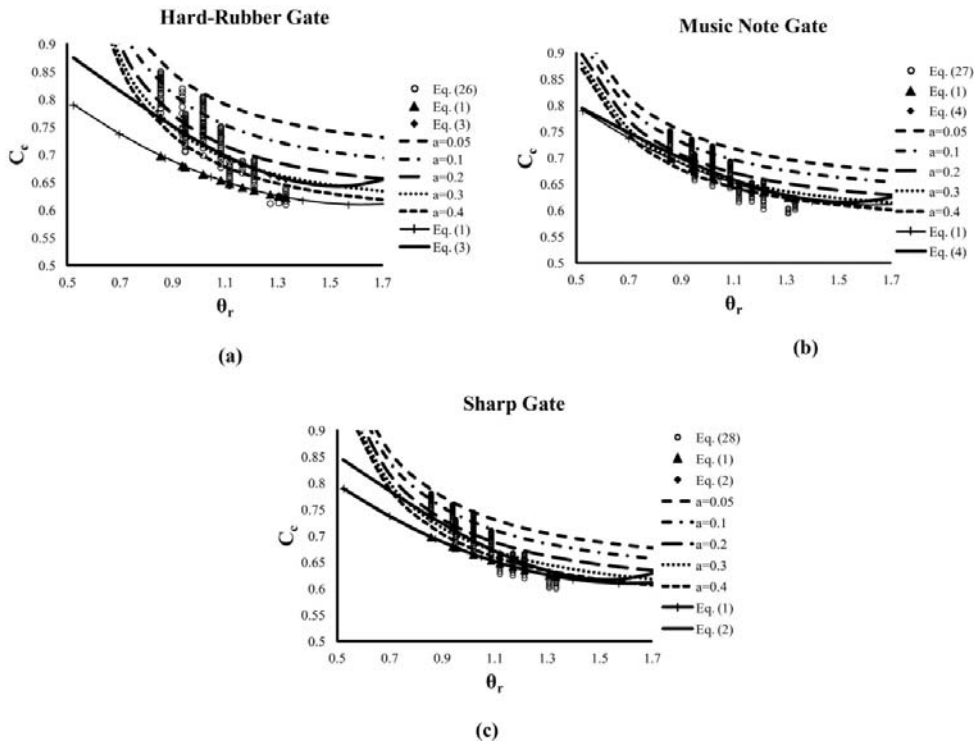


Fig. 10. Effects of relative gate opening and gate lip angle on contraction coefficient at free flow condition

Table 2 shows the values of the aforementioned parameters in Eq. (25). Denoting the pressure force behind the gate, the contraction coefficient under free flow conditions can be calculated from Eq. (13). Figure 10 shows the effects of gate lip angle, gate seal type and relative gate opening on the contraction coefficient under free flow condition. The obtained values of contraction coefficient from Eq. (13), follow the regression relations below:

$$\delta_{(Hard)} = 0.116\theta_r^{-2.425} - 5.099a^{0.011} + 5.634 \tag{26}$$

$$\delta_{(Music)} = 0.091\theta_r^{-1.842} - 0.281a^{0.176} + 0.806 \tag{27}$$

$$\delta_{(Sharp)} = 0.115\theta_r^{-1.89} - 0.236a^{0.226} + 0.755 \tag{28}$$

Table 2 . The proposed values for parameters in Eq. (25)

Type	A	B	C
Hard-Rubber	0.511	-0.759	-2.836
Music Note	0.513	-0.765	-2.706
Sharp	0.512	-0.789	-2.749

The above equations estimate the contraction coefficient related with relative gate opening and gate lip angle. Meanwhile, Eqs. (2),(3),(4) only considered the effect of gate lip angle. It is noteworthy to mention that the proposed equation is reliable only for  $0.055 \leq a \leq 0.799, 0.855 \leq \theta_r \leq 1.332$ . It can be seen from Fig. 10 that the contraction coefficient decreases with gate lip angle which matches what was reported by several previous researchers (Toch [10], Tel [12], and Wahl [1]). However, overlooking the effect of relative gate opening can raise considerable deviations in estimating the contraction coefficient. Figure 11 compares the effects of gate seal type on the contraction coefficient for a certain value of relative gate opening. Under a special condition, Hard-Rubber gates have a larger contraction coefficient than Sharp and Music Note gates have the smallest value, justified by Wahl [1]. Also, ignoring the effect of relative gate opening in Wahl’s [1] method ( Eqs. 2, 3, 4) and Toch’s [10] equation (Eq. (1)) reduces the contraction coefficient compared to the proposed method.

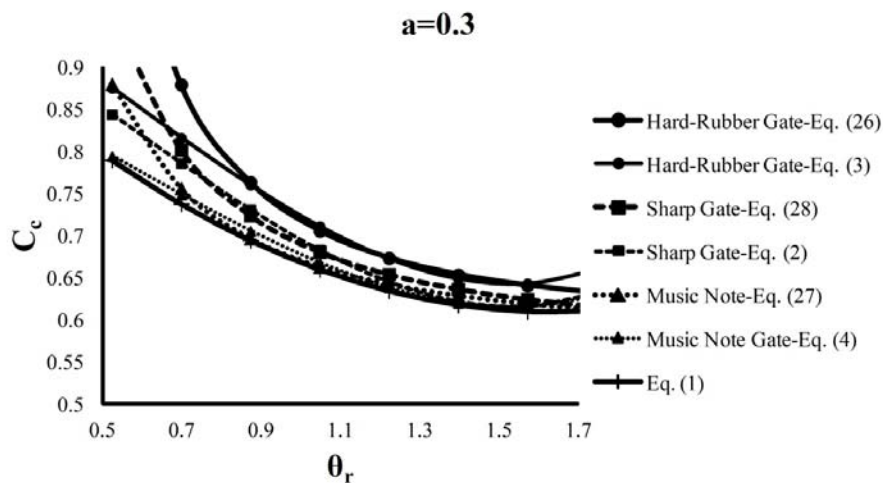


Fig. 11. Effects of gate seal type on contraction coefficient at free flow condition

The contraction coefficient can be used for estimating the discharge coefficient. Determining the contraction coefficient from Eqs. (26), (27), (28) and using Eq. (15), one can estimate the discharge coefficient under free flow conditions. Figure 12 compares the discharge coefficient calculated from this method by the data from Buyalski [11]. It can be seen that using the proposed methods by Toch [10], Tel [12] and Wahl [1], overestimates the discharge coefficient. Also, using Eqs. (26),(27),(28) this parameter can be more precisely obtained.

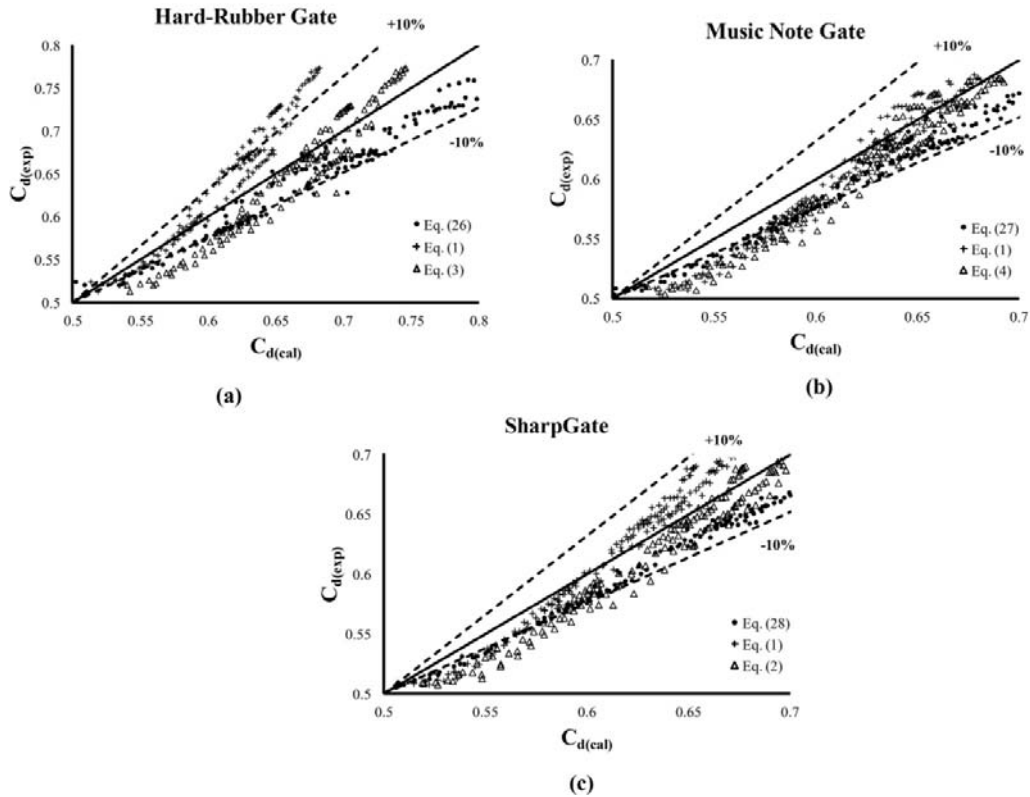


Fig. 12. Application of contraction coefficient for estimation of the discharge coefficient at free flow condition

For submerged flow under radial gates, the variation of the contraction coefficient can be determined using a similar procedure for sluice gates. Employing Buyalski's [11] data for any gate type, the variation of  $k$  with  $X$  can be determined (refer to Fig. 13):

$$k = a_1 - a_2 \cdot e^{-a_3 \cdot X^{-a_4}} \tag{29}$$

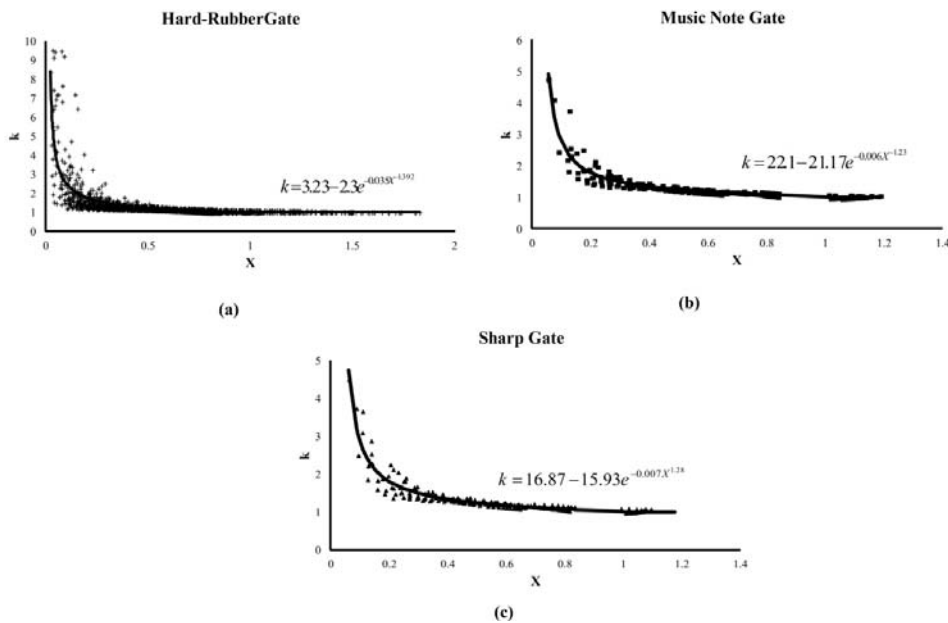


Fig. 13. General variation of  $k$  values with  $X$  for three types of radial gate

In fact, the parameters in Eq. (29) are functions of gate seal type and gate lip angle. Since there is not enough data on gate lip angles, one can only consider the effects of relative submergence and relative opening on the contraction coefficient. Similar to the free flow condition, Hard-Rubber gates have larger contraction coefficient values than Sharp and Music Note gates. Figure 14 shows variation of the contraction coefficient with relative opening and relative submergence under submerged flow conditions. It is shown that the contraction coefficient can be increased or decreased with relative submergence which was previously explained.

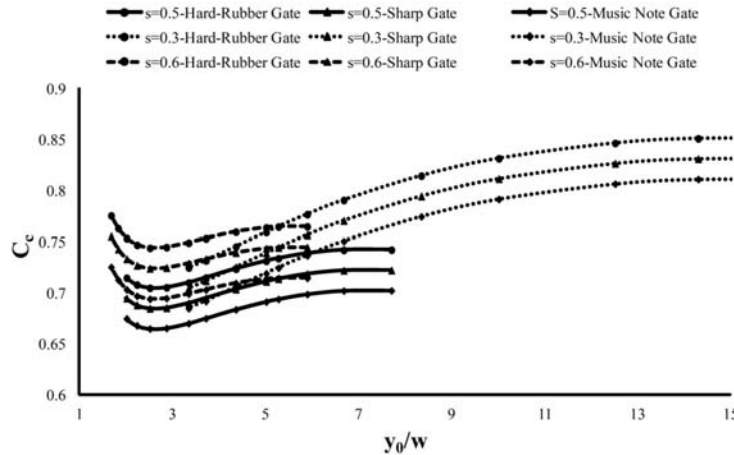


Fig. 14. General variation of contraction coefficient with relative gate opening, relative submergence and gate seal type

#### 4. CONCLUSION

This paper reports a theoretical method to determine the contraction coefficient affecting the flow from the gates. It was found that:

- 1- At free flow, the contraction coefficient factor of sluice gate tends to initially decrease with relative opening and then after reaching to its minimum value of  $\frac{w}{y_0} \approx 0.4$ , increases.
- 2- Under submerged flow conditions, the contraction coefficient of sluice and radial gates will either increase or decrease depending on the level of flow submergence.
- 3- Based on the suggested relationship for contraction coefficient, a theoretical relation is developed to estimate the discharge coefficient under free and submerged flow conditions with acceptable accuracy.
- 4- The contraction coefficient under free flow conditions is affected by gate seal type, gate lip angle and relative gate opening.
- 5- Under a special condition, Hard-Rubber gates have a larger contraction coefficient than Sharp and Music Note gates have the smallest value.
- 6- Ignoring the effect of relative gate opening in Wahl's [1] and Toch's [10] equations, reduces the contraction coefficient compared to the proposed method.

#### NOMENCLATURE

- $a$  relative gate opening ( $a = \frac{w}{y_0}$ )  
 $b$  gate width  
 $a_1, a_2, a_3, a_4$  parameters in Eq. (29)  
 $C_c$  contraction coefficient

$C_d$	discharge coefficient
$F_{p1}$	forces due to hydrostatic pressure at upstream section
$F_{p2}$	forces due to hydrostatic pressure at downstream section
$F_{g1}$	forces acting on upstream face of the gate
$F_{g2}$	forces acting on downstream face of the gate
$F_c$	force due to deviation from hydrostatic pressure distribution
$g$	acceleration due to gravity
$h_p(z)$	effective energy head at upstream face of the gate and any depth ( $z$ ) from the bed
$h_{pg(max)}$	maximum effective energy head at upstream face of the gate with free flow
$I$	integration of pressure head behind at upstream face of the gate with free flow
$I'$	integration of pressure head behind at upstream face of the gate with submerged flow
$k$	factor of pressure force at upstream face of the gate at submerged flow
$p(z)$	pressure at upstream face of the gate and any depth ( $z$ ) from the bed
$Q$	flow discharge
$q$	discharge per unit width of the gate
$s$	relative submergence ( $s = \frac{y_3}{y_0}$ )
$w$	gate opening
$Y$	Trunnion pin height
$y_0$	upstream flow depth
$y_1$	thickness of the vena contraction
$y_3$	downstream depth (immediately downstream of the gate)
$X$	relative maximum pressure head behind sluice gate
$\beta$	dimensionless function of pressure distribution behind the gate in free flow
$\beta'$	dimensionless function of pressure distribution behind the gate in submerged flow
$\gamma$	specify weight
$\eta$	correction factor for pressure distribution in vena contraction
$\kappa$	1 for submerged flow (0 for free flow)
$\theta^\circ$	gate lip angle (in degree)
$\theta_r$	gate lip angle (in radian)
$\rho$	mass density

## REFERENCES

1. Wahl, T. L. (2005). Refined energy correction for calibration of submerged radial gates. *Journal of Irrigation and Drainage Engineering, ASCE*, Vol. 131, No. 6, pp. 457–466.
2. Henry, R. (1950). Discussion to ‘On submerged jets’. *Transactions of the American Society of Civil Engineers*, Vol. 115, pp. 687–694.
3. Rajaratnam, N. & Subramanya, K. (1967). Flow equation for the sluice gate. *Journal of Hydraulic Divisions, ASCE*, Vol. 93, No. 4, pp. 57-77.
4. Swamee, P. (1992). Sluice gate discharge equations. *Journal of Irrigation and Drainage Engineering, ASCE*, Vol. 118, No. 1, pp. 56–60.
5. Belaud, G., Cassan, L. & Baume, J. P. (2009). Calculation of Contraction Coefficient under Sluice Gates and Application to Discharge Measurement. *Journal of Hydraulic Engineering, ASCE*, Vol. 135, No. 12, pp. 1086-1091.

6. Lozano, D., Mateos, L., Merkley, G. P. & Clemmens, A. J. (2009). Field calibration of submerged sluice gates in irrigation canals. *Journal of Irrigation and Drainage Engineering, ASCE*, Vol. 135, No. 6, pp. 763-772.
7. Habibzadeh, A., Vatankeh, A. R. & Rajaratnam, N. (2011). Role of energy loss on discharge characteristics of sluice gates. *Journal of Hydraulic Engineering, ASCE*, Vol. 137, No. 9, pp. 1079-1084.
8. Cassan, L. & Belaud, G. (2012). Experimental and numerical investigation of flow under sluice gates. *Journal of Hydraulic Engineering, ASCE*, Vol. 138, No. 4, pp. 367-373.
9. Metzler, D. E. (1948). A model study of Tainter gate operation. *MSc. thesis*, Iowa State University, Iowa City, Iowa.
10. Toch, A. (1955). Discharge characteristics of Tainter gates. *Transactions of the American Society of Civil Engineers*, Vol. 120, pp. 290-300.
11. Buyalski, C. P. (1983). Discharge algorithms for canal radial gates. *Research Report REC-ERC-83-9, United States Bureau of Reclamation*, Denver.
12. Tel, J. (2000). Discharge relations for radial gates. *MSc. thesis*, Delft Technical University, Delft, The Netherlands.
13. Clemmens, A. J., Strelkoff, T. S. & Replogle, J. A. (2003). Calibration of submerged radial gates. *Journal of Hydraulic Engineering, ASCE*, Vol. 129, No. 9, pp. 680-687.
14. Shahrokhnia, M. A. & Javan, M. (2003). Estimation of Radial Gate's Discharge Coefficient. *Journal of Hydraulics*, Vol. 1, No. 1, pp. 1-11 (In Persian).
15. Shahrokhnia, M. A. & Javan, M. (2006). Dimensionless stage-discharge relationship in radial gates. *Journal of Irrigation and Drainage Engineering, ASCE*, Vol. 132, No. 2, pp. 180-184.
16. Von Mises, R. (1917). Berechnung von Ausfluß und Ueberfallzahlen. *Zeitschrift des Vereines deutscher Ingenieure*, Berlin, Germany (in German).
17. Benjamin, T. B. (1956). On the flow in channels when rigid obstacles are placed in the stream. *Journal of Fluid Mechanics*, Vol. 1, pp. 227-248.
18. Lin, C. H., Yen, J. F. & Tsai, C. T. (2002). Influence of sluice gate contraction coefficient on distinguishing condition. *Journal of Irrigation and Drainage Engineering, ASCE*, Vol. 128, No. 4, pp. 249-252.
19. Ghadampour, Z., Talebbeydokhti, N., Hashemi, M. R., Nikseresht, A. H. & Neill, S. P. (2013). Numerical Simulation of Free Surface Mudflow Using Incompressible SPH. *Iranian Journal of Science and Technology, Transactions of Civil Engineering*, Vol. 37, No. C1, pp. 77-95.
20. Roth, A. & Hager, W. (1999). Underflow of standard sluice gate. *Experiments in Fluids*, Vol. 27, pp. 339-350.
21. Sepulveda, C. (2007). Instrumentation, model identification, and control of an experimental irrigation canal. *PhD Thesis*, Barcelona, Spain: Department of Hydraulic, Maritime and Environmental Engineering, Technical University of Catalonia.